

AUTOMATIC LANDMARK TRACKING APPLIED TO OPTIMIZE BRAIN CONFORMAL MAPPING

Lok Ming Lui, Yalin Wang, Tony F. Chan

University of California, Los Angeles
Department of Mathematics
{malmlui, ylwang, chan}@math.ucla.edu

Paul M. Thompson

UCLA School of Medicine
Laboratory of Neuroimaging,
Department of Neurology
thompson@loni.ucla.edu

ABSTRACT

Important anatomical features on the cortical surface are usually represented by landmark curves, called sulcal/gyral curves. Manual labeling of these landmark curves is time-consuming, especially when a large dataset is analyzed. In this paper, we propose a method to trace the landmark curves on the cortical surfaces automatically based on the principal directions of the local Weingarten matrix. Based on a global conformal parametrization of the cortical surface, our method adjusts the landmark curves iteratively on the spherical or rectangular parameter domain of the cortical surface along the principal direction field, using umbilic points of the surface as anchors. The landmark curves can then be mapped back onto the cortical surface. To speed up the iterative scheme, we obtain a good initialization by extracting the high curvature regions on the cortex using the Chan-Vese segmentation method, which solves a PDE on the manifold using our global conformal parametrization technique. Experimental results show that the landmark curves detected by our algorithm closely resemble the same curves labeled manually. We applied these automatically labeled landmark curves to build average cortical surfaces with an optimized brain conformal mapping method. Experimental results show that our method can help in automatically matching cortical surfaces of the brain across subjects.

1. INTRODUCTION

Finding important feature points or curves on anatomical surfaces, such as the sulcal/gyral curves of the cortex, is an important problem in medical imaging. It is extremely time-consuming to label these landmark curves manually, especially when data large dataset must be analyzed. An automatic or semi-automatic way to detect these feature curves would be invaluable. In this paper, we propose a method to trace the landmark curves on the cortical surfaces automatically. Given a global conformal parametrization of the cortical surface, we fix two endpoints, called the anchor points, based on umbilic points of the curvature field. We then trace the landmark curve by iteratively adjusting its path in the spherical or rectangular parameter domain of the cortex, along one of the two principal direction fields. Using the parameterization, the landmark curves can be mapped back onto the cortical surface in 3D. To speed up the iterative scheme, we propose a method to obtain a good initialization by extracting high curvature regions on the cortical surface using the Chan-Vese segmentation method[1]. This involves solving a PDE (Euler-Lagrange equation) on the cortical manifold using the global conformal parametrization. Finally, we used these automatic labelled landmark curves to created an optimized brain conformal mapping, which can match important anatomical features across subjects. This is based on the minimization of a combined energy functional $E_{new} = E_{harmonic} + \lambda E_{landmark}$.

2. PREVIOUS WORK

Automatic detection of sulcal landmarks on the cortical surface has been intensively studied by several research groups. Prince et al. [2] proposed a method to automatically segment major cortical sulci on the outer brain boundary. This is based on a statistical shape model, which includes a network of deformable curves on the unit sphere, and seeks geometric features such as high curvature regions. It then labels these features via a deformation process that is constrained within a spherical map of the outer brain boundary. Lohmann et al. [3] proposed an algorithm that automatically detects and attributes neuroanatomical names to the major cortical folds by applying image analysis methods to human brain MRI data. Sulcal basins are segmented using a region growing approach. Zeng et al. [4] proposed a method to automatic intrasulcal ribbon finding, by segmenting the cortex using coupled surfaces in a level set formulation, treating the outer cortical surface as the zero level set of a higher-dimensional distance function. By using the distance function, they formulated the sulcal ribbon finding problem in terms of level set-based surface deformations. Khanuja et al. [5] used dynamic programming to generate length-minimizing geodesics and curves of extremal curvature on the neocortex of the Macaque and the Visible Human. Subsoll [6] used the principal curvatures and "crest lines" to characterize sulcal/gyral shape and location, following the valleys and crests of the cortical surfaces. Rettman et al. [7] used watersheds on the cortical surface to automatically segment sulcal regions, followed by an atlas-based method assigned labels to the main sulci. Riviere et al. [8] and Mangin et al. [9] use a Markov Random Field model, called an attributed relational graph, to assign labels to a graph-based model of connected sulcal surfaces in 3D.

Optimization of surface diffeomorphisms by landmark matching has been studied intensively. Gu et al. [10] proposed to optimize the conformal parametrization of a surface by applying an optimal Möbius transformation to minimize a landmark mismatch energy. The resulting parameterization remains conformal. Glaunes et al. [11] generated large deformation diffeomorphisms of the sphere onto itself, given the displacements of a finite set of template landmarks. The diffeomorphism obtained can match the geometric features very well, although the resulting mapping is not generally conformal. Tosun et al. [12] proposed a more automated mapping technique that results in good sulcal alignment across subjects, by combining watershed segmentation, iterated closest point registration, optical flow to match scalar fields in the cortical parameter space, and inverse stereographic projection.

3. BASIC MATHEMATICAL THEORY

In this section, we will briefly review some basic mathematical definitions.

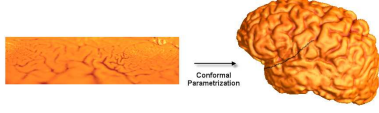


Fig. 1. Conformal parametrization of the cortical surface via a mapping onto a 2D rectangle.

Firstly, a diffeomorphism $f : M \rightarrow N$ is a *conformal mapping* if it preserves the first fundamental form up to a scaling factor (the conformal factor). Mathematically, this means that $ds_M^2 = \lambda f^*(ds_N^2)$, where ds_M^2 and ds_N^2 are the first fundamental form on surfaces M and N , respectively and λ is the conformal factor [13].

Next, we give a brief overview of curvatures on a Riemann surface. The normal curvature κ_n of a Riemann surface in a given direction is the reciprocal of the radius of the circle that best approximates a normal slice of the surface in that direction, which varies in different directions. It follows that:

$$\kappa_n = \mathbf{v}^T \mathbb{I} \mathbf{v} = \mathbf{v}^T \begin{pmatrix} e & f \\ f & g \end{pmatrix} \mathbf{v}$$

for any tangent vector \mathbf{v} . \mathbb{I} is called the Weingarten matrix and is symmetric. Its eigenvalues and eigenvectors are called *principal curvatures* and *principal directions* respectively. The sum of the eigenvalues is the *mean curvature*. A point on the Riemann surface at which the Weingarten matrix has the same eigenvalues is called an *umbilic point* [14].

4. ALGORITHM

In this section, we discuss our algorithm for automatic landmark tracking and how it is applied.

4.1. Computation of conformal parameterization

For a diffeomorphism between two genus zero (closed) surfaces, a map is conformal if and only if it minimizes the harmonic energy, $E_{harmonic}$ [10]. A conformal map can thus be obtained by minimizing the harmonic energy. However, this is not true for surfaces of genus one or higher.

For high genus surfaces, Gu et. al [15] proposed an efficient approach to parameterize surfaces conformally using a set of connected 2D rectangles. They compute a holomorphic 1-form on the Riemann surface, using concepts from homology and cohomology group theory, and Hodge theory.

With this method, we can compute a conformal parametrization from any given surface onto a 2D domain. (See Figure 1) [16]

4.2. Computation of principal direction fields from the global conformal parametrization

Denote the cortical surface by C . Let $\phi : D \rightarrow C$ be the global conformal parametrization of C where D is a rectangular parameter domain. Let λ be the conformal factor of ϕ . Following Rusinkiewicz's work [17], we can compute the principal directions, and represent them on the parameter domain D . This is based on the following three steps:

Step 1: Per-Face Curvature Computation

The Weingarten matrix is defined in terms of the directional derivatives of the normal vector \mathbf{n} :

$$\mathbb{I} = (D_u \mathbf{n}, D_v \mathbf{n}) = \begin{pmatrix} \frac{\partial \mathbf{n}}{\partial u} \cdot \mathbf{u} & \frac{\partial \mathbf{n}}{\partial u} \cdot \mathbf{v} \\ \frac{\partial \mathbf{n}}{\partial u} \cdot \mathbf{v} & \frac{\partial \mathbf{n}}{\partial v} \cdot \mathbf{v} \end{pmatrix}$$

where $\mathbf{u} = \begin{pmatrix} \frac{1}{\sqrt{\lambda}} \\ 0 \end{pmatrix}$ and $\mathbf{v} = \begin{pmatrix} 0 \\ \frac{1}{\sqrt{\lambda}} \end{pmatrix}$ are the directions of an orthonormal coordinate system for the tangent plane (represented in the parameter domain D).

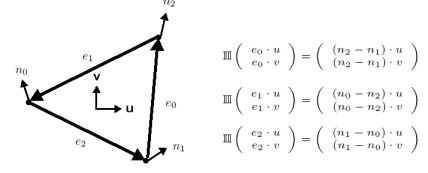


Fig. 2. A single face (triangle) of the triangulated mesh.

Simple checking gives: $\mathbb{I} \mathbf{s} = D_s \mathbf{n}$, which is the derivative of the normal in the direction \mathbf{s} - this is also a vector in the tangent plane. Given a triangulation of the Riemann surface, we can approximate the Weingarten matrix \mathbb{I} for each face (triangle).

For a triangle with three well-defined directions (edges) together with the differences in normals in those directions (Refer to Figure 2). We have:

$$\mathbb{I} \begin{pmatrix} e_0 \cdot \mathbf{u} \\ e_0 \cdot \mathbf{v} \end{pmatrix} = \begin{pmatrix} (n_2 - n_1) \cdot \mathbf{u} \\ (n_2 - n_1) \cdot \mathbf{v} \end{pmatrix}; \mathbb{I} \begin{pmatrix} e_1 \cdot \mathbf{u} \\ e_1 \cdot \mathbf{v} \end{pmatrix} = \begin{pmatrix} (n_0 - n_2) \cdot \mathbf{u} \\ (n_0 - n_2) \cdot \mathbf{v} \end{pmatrix};$$

$$\mathbb{I} \begin{pmatrix} e_2 \cdot \mathbf{u} \\ e_2 \cdot \mathbf{v} \end{pmatrix} = \begin{pmatrix} (n_1 - n_0) \cdot \mathbf{u} \\ (n_1 - n_0) \cdot \mathbf{v} \end{pmatrix}$$

This gives a set of linear constraints on the elements of the Weingarten matrix, which can be determined using the least square method.

Step 2: Coordinate system Transformation

After we compute the Weingarten matrix on each face in the (u_f, v_f) coordinate system, we can average it with contributions from adjacent triangles. Suppose that each vertex p has its own orthonormal coordinate system (u_p, v_p) . We have to transform the Weingarten matrix tensor into the vertex coordinate frame. The first component of \mathbb{I} , expressed in the (u_p, v_p) coordinate system, can be found as:

$$e_p = u_p^T \mathbb{I} u_p = (1, 0) \begin{pmatrix} e_p & f_p \\ f_p & g_p \end{pmatrix} (1, 0)^T$$

Thus, $e_p = (u_p \cdot u_f, u_p \cdot v_f) \mathbb{I} (u_p \cdot u_f, u_p \cdot v_f)^T$

We can find f_p and g_p similarly.

Step 3: Weighting

Another question is: how much of the face curvature should be accumulated at each vertex? For each face f which is adjacent to the vertex p , we take the weighting $w_{f,p}$ to be the area of f divided by the squares of the lengths of the two edges that touch the vertex p .

4.3. Variational method for landmark tracking

Given the principal direction field $\vec{V}(t)$ with smaller eigenvalues on the cortical surface C , we propose a variational method to trace the sulcal landmark curve iteratively, after fixing two anchor points (a & b) on the sulci. Let $\phi : D \rightarrow C$ be the conformal parametrization of C , $\langle \cdot, \cdot \rangle$ to be its Riemannian metric and λ to be its conformal factor. We propose to locate a curve $\vec{c} : [0, 1] \rightarrow C$ with endpoints a and b , that minimizes the following energy functional:

$$E_{principal}(\vec{c}) = \int_0^1 \left| \frac{\vec{c}'}{\sqrt{\langle \vec{c}', \vec{c}' \rangle_M}} - \vec{\nabla} \circ \vec{c} \right|_M^2 dt = \int_0^1 \lambda \left| \frac{\vec{\gamma}'}{\sqrt{\lambda \langle \vec{\gamma}', \vec{\gamma}' \rangle}} - \vec{\nabla} \circ \vec{\gamma} \right|^2 dt$$

$$= \int_0^1 \left| \frac{\vec{\gamma}'}{|\vec{\gamma}'|} - \sqrt{\lambda} \vec{\nabla} \circ \vec{\gamma} \right|^2 dt = \int_0^1 \left| \frac{\vec{\gamma}'}{|\vec{\gamma}'|} - \vec{G}(\vec{\gamma}) \right|^2 dt$$

where $\vec{\gamma} = \vec{c} \circ \phi^{-1} : [0, 1] \rightarrow D$ is the corresponding iteratively defined curve on the parameter domain; $\vec{G}(\vec{\gamma}) = \sqrt{\lambda(\vec{\gamma})} \vec{V}(\vec{\gamma})$; $|\cdot|_M^2 = \langle \cdot, \cdot \rangle_M$ and $|\cdot|$ is the (usual) length defined on D . By minimizing the energy E , we minimize the difference between the tangent vector field along the curve and the principal direction field

\vec{V} . The resulting minimizing curve is the curve that is closest to the curve traced along the principal direction.

Let: $\vec{G} = (G_1, G_2, G_3)$; $\vec{K} = (K_1, K_2, K_3) = \frac{\vec{\gamma}'}{|\vec{\gamma}'|} - \vec{G}(\vec{\gamma})$

$\vec{L}_1 = \frac{(1,0,0)}{|\vec{\gamma}'|} - \frac{\gamma_1 \vec{\gamma}}{|\vec{\gamma}'|^3}$; $\vec{L}_2 = \frac{(0,1,0)}{|\vec{\gamma}'|} - \frac{\gamma_2 \vec{\gamma}}{|\vec{\gamma}'|^3}$; $\vec{L}_3 = \frac{(0,0,1)}{|\vec{\gamma}'|} - \frac{\gamma_3 \vec{\gamma}}{|\vec{\gamma}'|^3}$

We can locate the landmark curves iteratively using the steepest descent algorithm: $\frac{d\vec{\gamma}}{dt} = \sum_{i=1}^3 [K_i \vec{L}_i]' + K_i \nabla G_i$

4.4. Landmark hypothesis by Chan-Vese Segmentation

In order to speed up the iterative scheme, we decided to obtain a good initialization by extracting the high curvature regions on the cortical surface using the Chan-Vese (CV) segmentation method [1]. We can extend the CV segmentation on \mathbb{R}^2 to any arbitrary Riemann surface M such as the cortical surface.

Let $\phi : \mathbb{R}^2 \rightarrow M$ be the conformal parametrization of the surface M .

We propose to minimize the following energy functional:

$$F(c_1, c_2, \psi) = \int_M (u_0 - c_1)^2 H(\psi) dS + \int_M (u_0 - c_2)^2 (1 - H(\psi)) dS + \nu \int_M |\nabla_M H(\psi)|_M dS,$$

where $\psi : M \rightarrow \mathbb{R}$ is the level set function and $|\cdot|_M = \sqrt{\langle \cdot, \cdot \rangle}$.

With the conformal parametrization, we have:

$$F(c_1, c_2, \psi) = \int_{\mathbb{R}^2} \lambda(u_0 \circ \phi - c_1)^2 H(\psi \circ \phi) dx dy + \int_{\mathbb{R}^2} \lambda(u_0 \circ \phi - c_2)^2 (1 - H(\psi \circ \phi)) dx dy + \nu \int_{\mathbb{R}^2} \sqrt{\lambda} |\nabla H(\psi \circ \phi)| dx dy$$

For simplicity, we let $\zeta = \psi \circ \phi$ and $w_0 = u_0 \circ \phi$. Fixing ζ , we must have:

$$c_1(t) = \frac{\int_{\Omega} w_0 H(\zeta(t, x, y)) \lambda dx dy}{\int_{\Omega} H(\zeta(t, x, y)) \lambda dx dy}; c_2(t) = \frac{\int_{\Omega} w_0 (1 - H(\zeta(t, x, y))) \lambda dx dy}{\int_{\Omega} (1 - H(\zeta(t, x, y))) \lambda dx dy}$$

Fixing c_1, c_2 , the Euler-Lagrange equation becomes:

$$\frac{\partial \zeta}{\partial t} = \lambda \delta(\zeta) \left[\nu \frac{1}{\lambda} \nabla \cdot (\sqrt{\lambda} \frac{\nabla \zeta}{\|\nabla \zeta\|}) - (w_0 - c_1)^2 + (w_0 - c_2)^2 \right]$$

Now, the sulcal landmarks on the cortical surface lie at locations with relatively high curvature. To formulate the CV segmentation, we can consider the intensity term as being defined by the mean curvature. Sulcal locations can then be circumscribed by first extracting out the high curvature regions. Fixing two anchor points inside the extracted region, we can get a good initialization of the landmark curve by looking for a shortest path inside the region that joins the two points. Also, we can consider the umbilic points inside the region as anchor points. By definition, an umbilic point on a manifold is a location where the two principal curvatures are the same. Therefore, we can fix the anchor points inside the region by extracting regions with a small difference in principal curvatures.

5. OPTIMIZATION OF BRAIN CONFORMAL PARAMETRIZATION

In brain mapping research, cortical surface data are often mapped to a parameter domain such as a sphere, providing a common coordinate system for data integration [18, 19]. Conformal mapping offers a convenient way to parameterize the genus zero cortical surfaces of the brain onto the sphere [10]. To compare cortical surfaces

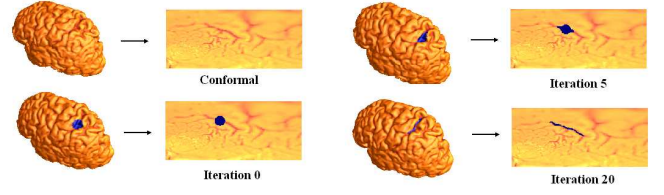


Fig. 3. Sulcal curve extraction on the cortical surface by Chan-Vese segmentation. As iterations proceed, the contour is evolved to the deep sulcal region.

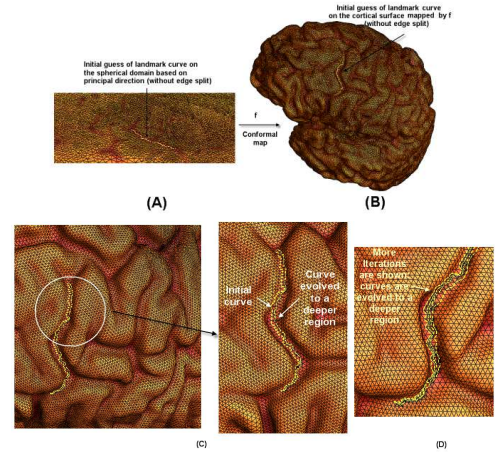


Fig. 4. Automatic landmark tracking using a variational approach. In (a), we trace the landmark curves in the parameter domain along the edges whose directions are closest to the principal direction field. The corresponding landmark curves on the cortical surface is shown in (b). This gives a good initialization for our variational method to locate landmarks. (c) & (d) show the landmark curves after different numbers of iterations.

more effectively, it is desirable to adjust the conformal parameterizations to match specific anatomical features on the cortical surfaces as far as possible. As an application of our automatic landmark tracking algorithm, we use the automatically labelled landmark curves to generate an optimized conformal mapping on the surface, in the sense that homologous features across subjects are caused to lie at the same parameter locations in a conformal grid. This matching of cortical patterns improves the alignment of data across subjects, e.g., when integrating functional imaging data across subjects, measuring brain changes, or making statistical comparisons in cortical anatomy. This is done by minimizing the compound energy functional $E_{new} = E_{harmonic} + \lambda E_{landmark}$, where $E_{harmonic}$ is the harmonic energy of the parameterization and $E_{landmark}$ is the landmark mismatch energy.

Suppose C_1 and C_2 are two cortical surfaces we want to compare. We let $f_1 : C_1 \rightarrow S^2$ be the conformal parameterization of C_1 mapping it onto S^2 . Let $\{p_i : [0, 1] \rightarrow S^2\}$ and $\{q_i : [0, 1] \rightarrow S^2\}$ be the automatic labelled landmark curves, represented on the parameter domain S^2 with unit speed parametrization, for C_1 and C_2 respectively. Let $h : C_2 \rightarrow S^2$ be any homeomorphism from C_2 onto S^2 . We define the landmark mismatch energy of h as: $E_{landmark}(h) = 1/2 \sum_{i=1}^n \int_0^1 \|h(q_i(t)) - f_1(p_i(t))\|^2 dt$, where the norm represents distance on the sphere. By minimizing this energy functional, the Euclidean distance between the corresponding landmarks on the sphere is minimized [20].

6. EXPERIMENTAL RESULTS

In one experiment, we tested our automatic landmark tracking algorithm on a set of left hemisphere cortical surfaces extracted from brain MRI scans, acquired from normal subjects at 1.5 T (on a GE Signa scanner). In our experiments, 6 landmarks were automatically located on cortical surfaces.

Figure 3, shows how we can effectively locate the initial landmark guess areas on the cortical surface using the Chan-Vese segmentation. Notice that the contour evolved to the deep sulcal region.

Our variational method to locate landmark curves is illustrated in Figure 4. With the initial guess given by the Chan-Vese model (we choose the two extreme points in the located area as the anchor points), we trace the landmark curves iteratively based on the principal direction field. In Figure 4 (a), we trace the landmark curves on the parameter domain along the edges whose directions are closest to the principal direction field. The corresponding landmark curves on the cortical surface are shown in Figure 4 (b). Figure 4 c & d show the landmark curves after different numbers of iterations. The curve evolves to a deeper sulcal region with each iteration.

To compare our automatic landmark tracing results with the manually labeled landmarks, we measured the Euclidean distance $E_{difference}$ (on the parameter domain) between the automatically and manually labelled landmark curves. Figure 5 shows the value of $E_{difference}$ at different iterations for different landmark curves. Note that the value becomes smaller as the iterations proceed. This means that the automatically labeled landmark curves more closely resemble those defined manually as the iterations continue.

Figure 6 illustrates an application of our automatic landmark tracking algorithm. We illustrate our idea of optimizing conformal mappings using the automatically traced landmark curves. Figure 6 (A) and (B) show two different cortical surfaces being mapped conformally to the sphere. Notice that the alignment of the sulcal landmark curves are not consistent across subjects. In Figure 6 (C), the same cortical surface in (B) is mapped to the sphere using our method. The landmark curves closely resemble those in (A), meaning that the landmark curves are more consistently aligned with our algorithm.

To visualize how well our algorithm can improve the alignment of key sulcal landmarks, we took the 3D vector average of the 15 surfaces re-parameterized using optimized conformal maps [20]. Figure 6 shows average surface maps from multiple subjects from different viewpoints. In (D) and (E), sulcal landmarks are clearly preserved inside the green circle where landmarks are automatically labeled. In (F), the sulcal landmarks are averaged out inside the green circle where no landmarks were automatically detected. This implies that our algorithm can help improve the alignment of the important anatomical features, which should greatly assist in multi-subject averaging and statistical analysis of cortical data.

7. CONCLUSION AND FUTURE WORK

In this paper, we proposed a variational method to automatically trace landmark curves on cortical surfaces, based on the principal directions. To accelerate the iterative scheme, we initialized the curves by extracting high curvature regions using Chan-Vese segmentation. This involves solving a PDE on the cortical manifold. The landmark curves detected by our algorithm closely resembled those labeled manually. Finally, we used the automatically labeled landmark curves to create an optimized brain conformal mapping, which matches important anatomical features across subjects. Surface averages from multiple subjects showed that our computed maps can consistently align key anatomic landmarks. In future, we will perform a more exhaustive quantitative analysis of our algorithm's per-

Difference between the two landmarks is measured by:

$$E_{difference} = \int_0^1 \|\vec{\tau}_{principal}(t) - \vec{\tau}_{manual}(t)\|^2 dt$$

	Central sulci landmark	Pre-central sulci landmark	Post-central sulci landmark
Iteration 0	1.28	1.05	1.33
Iteration 3	0.96	0.88	0.82
Iteration 6	0.82	0.78	0.73
Iteration 10	0.38	0.27	0.28

Fig. 5. Numerical comparison between automatically labeled landmarks and manually labeled landmarks by computing the Euclidean distance $E_{difference}$ (in the parameter domain) between the automatically and manually labeled landmark curves.

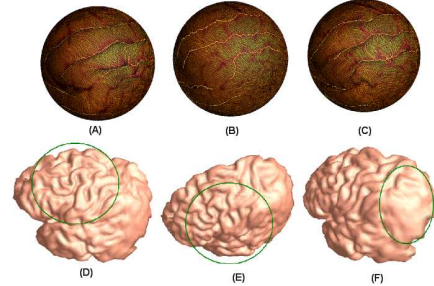


Fig. 6. Optimization of brain conformal mapping using automatic landmark tracking. In (A) and (B), two different cortical surfaces are mapped conformally to the sphere. In (C), we map one of the cortical surfaces to the sphere using our algorithm. (D), (E), (F) shows the average surface (for N=15 subjects) based on the optimized conformal re-parameterization using the variational approach. Except in (F), where no landmarks were defined automatically, the major sulcal landmarks are remarkably well defined, even in this multi-subject average.

formance, mapping errors and quantifying improved registration, across multiple subjects, on a regional basis.

8. REFERENCES

- [1] L.A. Vese et al., " *Intl J. of Comp. Vis.*, vol. 50, no. 3, pp. 271–293, 2002.
- [2] J. L. Prince et al., " *IEEE TMI*, vol. 21, no. 5, pp. 513–524, 2002.
- [3] G. Lohmann et al., " *IPMI*, vol. 1230, pp. 368–374, 1997.
- [4] X. Zeng et al., " *3rd MICCAI*, 1999.
- [5] N. Khaneja et al., " *IEEE PAMI*, vol. 20, no. 11, pp. 1260–1265, Nov. 1998.
- [6] G. Subsol, *Brain Warping*, chapter Crest Lines for Curve Based Warping, 1998.
- [7] M.E. Rettman et al., " *NeuroImage*, vol. 15, no. 2, pp. 329–344, 2002.
- [8] Y. Cointepas et al., " *NeuroImage*, vol. 13, no. 6, pp. S98, 2001.
- [9] J.-F. Mangin et al., " *Medical Image Analysis*, pp. 187–196, 2004.
- [10] X. Gu et al., " *IEEE TMI*, vol. 23, no. 8, pp. 949–958, Aug. 2004.
- [11] J. Glaunès et al., " *J. Maths. Imaging and Vision*, vol. 20, pp. 179–200, 2004.
- [12] D. Tosun et al., " *Med. Image Anal.*, vol. 8, no. 3, pp. 295–309, Sep. 2004.
- [13] R. Schoen and S.-T Yau, International Press, 1997.
- [14] R. Cipolla and P. J. Giblin, Cambridge University Press, 2000.
- [15] X. Gu and S.-T Yau, " *ACM Symp on Geom. Processing 2003*, 2003.
- [16] Y. Wang et al., " *10th IEEE ICCV*, pp. 1061–1066, 2005.
- [17] S. Rusinkiewicz, " *Symp. on 3D Data Processing, Vis., and Trans.*, 2004.
- [18] H.A. Drury et al., chapter Surface-based analyses of the human cerebral cortex, 1999.
- [19] B. Fischl et al., " in *Human Brain Mapping*, 1999, vol. 8, pp. 272–284.
- [20] L.M. Lui et al., " *VLSM, ICCV*, 2005.